

# HGAurban: Heterogeneous Graph Autoencoding for Urban Spatial-Temporal Learning

Qianru Zhang  
The University of Hong Kong  
Hong Kong  
zqrhku@connect.hku.hk

Xinyi Gao  
The University of Queensland  
Brisbane

Haixin Wang  
University of California, Los Angeles  
Los Angeles

Dong Huang  
National University of Singapore  
Singapore

Siu-Ming Yiu\*  
The University of Hong Kong  
Hong Kong

Hongzhi Yin†  
The University of Queensland  
Brisbane

## ABSTRACT

Spatial-temporal graph representations play a crucial role in urban sensing applications, including traffic analysis, human mobility behavior modeling, and citywide crime prediction. However, a key challenge lies in the noisy and sparse nature of spatial-temporal data, which limits existing neural networks' ability to learn meaningful region representations in the spatial-temporal graph. To overcome these limitations, we propose HGAurban, a novel heterogeneous spatial-temporal graph masked autoencoder that leverages generative self-supervised learning for robust urban data representation. Our framework introduces a spatial-temporal heterogeneous graph encoder that extracts region-wise dependencies from multi-source data, enabling comprehensive modeling of diverse spatial relationships. Within our self-supervised learning paradigm, we implement a masked autoencoder that jointly processes node features and graph structure. This approach automatically learns heterogeneous spatial-temporal patterns across regions, significantly improving the representation of dynamic temporal correlations. Comprehensive experiments across multiple spatiotemporal mining tasks demonstrate that our framework outperforms state-of-the-art methods and robustly handles real-world urban data challenges, including noise and sparsity in both spatial and temporal dimensions.

## ACM Reference Format:

Qianru Zhang, Xinyi Gao, Haixin Wang, Dong Huang, Siu-Ming Yiu, and Hongzhi Yin. 2025. HGAurban: Heterogeneous Graph Autoencoding for Urban Spatial-Temporal Learning. In *Proceedings of ACM Conference (Conference'17)*. ACM, New York, NY, USA, 10 pages. <https://doi.org/10.1145/nmnnnnn.nmnnnnn>

## 1 INTRODUCTION

As remote sensing technologies and large-scale computing infrastructures continue to provide an abundance of spatial-temporal

data, there is an increasing demand for robust spatial-temporal prediction frameworks in urban sensing applications. These applications include traffic analysis [4, 16, 20, 31–33, 39, 45, 47], as well as modeling human mobility behavior [6, 23, 42, 44]. Additionally, citywide crime prediction [1, 3, 19, 43, 46] is another important area of focus. A crucial aspect of developing effective spatial-temporal prediction frameworks lies in the accurate capture of spatial and temporal correlations between different geographical locations and time intervals. This ability ensures comprehensive insights into dynamic urban phenomena.

Researchers have introduced spatial-temporal graph neural networks (STGNNs) as a promising learning paradigm [13, 25, 27]. These networks are specifically designed to handle data with graph structures and have garnered significant attention due to their ability to capture multi-hop spatial and temporal dependencies. This is accomplished through the iterative propagation of messages among nodes, leveraging their knowledge of both spatial and temporal information. By employing this recursive message passing mechanism, STGNNs demonstrate exceptional proficiency in modeling intricate dependencies in spatial-temporal data. Their effectiveness lies in their capability to integrate and exploit the inherent structure and temporal dynamics of the data, enabling more accurate predictions and insightful analysis of various urban applications.

However, existing works in STGNNs have not adequately addressed the challenges of noise and sparsity in spatial-temporal data, which hinders the accurate modeling of dependencies. For instance, traffic data collected from sensors or GPS devices may contain outliers or missing values, leading to less relevant region connections and noisy signals. These noisy signals can negatively impact the performance of spatial-temporal prediction tasks, as they introduce irrelevant information and hinder the accurate modeling of dependencies. Besides, most existing solutions approach spatial-temporal prediction tasks in a supervised manner, relying on a sufficient amount of labeled data for training. However, spatial-temporal data is often sparsely labeled, especially for rare urban anomalies or events. This sparsity presents a significant challenge in building accurate prediction models. Thus, it becomes crucial to develop learning models that can effectively handle sparse labeled data and learn from limited samples for achieving accurate spatial-temporal predictions in real-world urban scenarios.

\*Corresponding author

†Corresponding author

Permission to make digital or hard copies of all or part of this work for personal or classroom use is granted without fee provided that copies are not made or distributed for profit or commercial advantage and that copies bear this notice and the full citation on the first page. Copyrights for components of this work owned by others than ACM must be honored. Abstracting with credit is permitted. To copy otherwise, or republish, to post on servers or to redistribute to lists, requires prior specific permission and/or a fee. Request permissions from [permissions@acm.org](mailto:permissions@acm.org).  
*Conference'17, July 2017, Washington, DC, USA*

© 2025 Association for Computing Machinery.  
ACM ISBN 978-x-xxxx-xxxx-x/YY/MM... \$15.00  
<https://doi.org/10.1145/nmnnnnn.nmnnnnn>

In light of these challenges, we propose **heterogeneous graph autoencoding for urban spatial-temporal learning (HGAurban)**. Our framework leverages multi-view spatial-temporal data and introduces a spatial-temporal heterogeneous graph neural encoder to capture region-wise dependencies. By considering both intra-view and inter-view data correlations, our model effectively models spatial-temporal patterns. Moreover, we propose a self-supervised learning paradigm that utilizes the mask mechanism to distill heterogeneous dependencies across observed regions in urban space. Specifically, we adopt the masked autoencoding mechanism on the node representations and graph structures to identify and emphasize the most relevant connections for prediction tasks. This enhances the learning process of implicit cross-region relations and improves the robustness of the model against noisy signals.

At the core of our approach is a generative spatial-temporal graph auto-encoder. This model learns to reconstruct both node features and the graph structure by utilizing the mask mechanism. By selectively masking certain regions in the input data during training, our model focuses on capturing the dependencies between regions and effectively reconstructing the missing or corrupted features and connections. This capability effectively overcomes the data sparsity by providing accurate self-supervisory signals to prioritize the most relevant information.

Our HGAurban framework has been extensively evaluated in diverse spatial-temporal mining tasks and compared against multiple region representation and GNN baselines. The results demonstrate the effectiveness and superiority of our proposed method in addressing the challenges associated with data noise and sparsity. We highlight the key contributions as follows:

- We place a strong emphasis on addressing the challenges of data noise in spatial-temporal prediction tasks. To achieve this, we introduce the superiority of self-supervised learning in region representation, incorporating the mask mechanism to enhance the robustness and generalization ability of our spatial-temporal heterogeneous graph neural architecture.
- We propose a spatiotemporal heterogeneous graph neural network that captures both intra-view and inter-view regional dependencies while modeling diverse spatiotemporal factors. To address data sparsity, we introduce a masked autoencoding mechanism that masks both node features and graph structures within the heterogeneous spatiotemporal graph, enabling the model to effectively explore inter-correlations among regions.
- We rigorously validate our HGAurban across a range of spatial-temporal mining tasks, conducting comprehensive comparisons with state-of-the-art baselines. Our method consistently achieves the best performance across three diverse tasks. The code is publicly available at <https://github.com/lizzyhku/HGAurban>.

## 2 METHODOLOGY

The framework of HGAurban is depicted in Figure 1, which addresses the task of reconstructing links and features of masked nodes using a mask mechanism based on generative self-supervised learning on the heterogeneous spatial-temporal graph. The HGAurban framework operates on the heterogeneous spatial-temporal graph  $\mathcal{G}$ , which incorporates various types of information, such as spatial, temporal, and attribute data. Our HGAurban employs an

encoder-decoder architecture. The encoder captures the underlying structure and derives meaningful representations from the heterogeneous spatiotemporal graph  $\mathcal{G}$ , while the decoder reconstructs the masked node features and graph links. By utilizing the mask mechanism, HGAurban learns to reconstruct the missing links and features of masked nodes, thereby capturing the correlations and dependencies. And the specific algorithm of HGAurban is shown in Algorithm 1.

### 2.1 Preliminaries

In our methodology, we employ a partitioning approach to divide the geographic area of a city (such as New York) into  $I$  spatial-regions. Each spatial-region is identified by an index, denoted as  $i$  (e.g.,  $r_i$ ). To capture a wide range of urban contextual information, we propose a region embedding framework that integrates multiple diverse data sources associated with the metropolitan space. These data sources are incorporated into HGAurban to generate enriched spatial-region representations, which are shown as follows.

**Region Point-of-Interests (POIs).** We create a POI matrix  $\mathbf{P} \in \mathbb{R}^{I \times C}$ , where  $C$  is the number of POI categories, to characterize the region’s urban functions (such as entertainment and health).

**Human Mobility Trajectories.** We create a matrix  $\mathbf{M} \in \mathbb{R}^{I \times T}$  utilizing human trajectory to accurately represent the dynamic urban flows between citywide zones, where  $T$  is the number of time slots. Individual human mobility traces are saved in this collection as  $(r_s, r_d, t_s, t_d)$ , where  $r_s$  and  $r_d$  denote source and destination regions, respectively, and  $t_s$  and  $t_d$  stand for timestamp data.

**Spatial Correlations.** We create a spatial matrix  $\mathcal{D} \in \mathbb{R}^{I \times I}$ . It is composed of region pairs like  $(r_s, r_d, d')$  whose geographical distances are less than a threshold  $\epsilon$ , where  $d'$  denotes the distance from the source node  $r_s$  to the destination node  $r_d$ .

**Problem Statement:** Given the spatial-temporal graph, denoted as  $\mathcal{G} = (\mathcal{V}, \mathcal{E})$ , where  $\mathcal{V}$  and  $\mathcal{E}$  are node set and edge set respectively.  $\mathcal{G}$  is built upon the POI matrix  $\mathcal{P}$ , the mobility matrix  $\mathbf{M}$  and the spatial matrix  $\mathcal{D}$ . The task of this work is to learn a function  $f$ , which maps each node of  $\mathcal{G}$  to the embedding space and reconstruct both the structure  $\mathbf{A} \in \mathbb{R}^{|\mathcal{V}| \times |\mathcal{V}|}$  and features  $\mathbf{X} \in \mathbb{R}^{|\mathcal{V}| \times D}$  of the input spatial-temporal graph  $\mathcal{G}$ . Meanwhile, the embedding space can effectively preserve the geographical and temporal connections between various locations and time slots, which is advantageous for a variety of urban sensing applications (e.g. traffic forecasting and crime prediction).

### 2.2 Embedding Layer

To incorporate the Point-of-Interest (POI) context into region embeddings, we have developed a POI context embedding layer that reflects the functional information of each region in the latent representation space. Inspired by the POI token embedding technique using Skip-gram [24], we input the region-specific POI vector into the Skip-gram model [2] for POI context embedding. Subsequently, we concatenate the region-specific POI embeddings to generate POI-aware representations:  $\mathbf{E} = \text{MLP}(\text{Skip-gram}(\mathcal{P}))$ .

Here, we employ a Multi-Layer Perceptron (MLP) for the embedding projection. The embedding table  $\mathbf{E} \in \mathbb{R}^{I \times d}$  represents the embeddings for all regions, where  $d$  is the hidden dimensionality. Each region’s embedding  $\mathbf{e}_i$  captures the region-specific POI contextual information in the latent semantic space. To incorporate

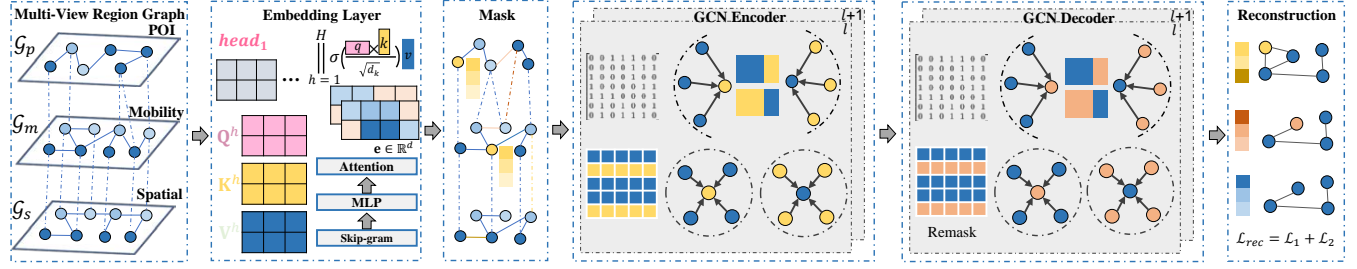


Figure 1: Architecture of our HGAurban region representation model with graph masked autoencoder.

region interactions within our POI embedding layer, we introduce a region-wise self-attention mechanism given by:

$$\mathbf{e}_i = \left\| \sum_{h=1}^H \sum_{j=1}^I \alpha_{i,j}^h \cdot \mathbf{v}^h \mathbf{e}_j; \quad \alpha_{i,j}^h = \delta \left( \frac{(\mathbf{Q}^h \mathbf{e}_i)^\top (\mathbf{K}^h \mathbf{e}_j)}{\sqrt{d/H}} \right) \quad (1)$$

Here,  $\mathbf{V}^h$ ,  $\mathbf{Q}^h$ , and  $\mathbf{K}^h \in \mathbb{R}^{d/H \times d}$  correspond to the value, query, and key transformations for the  $h$ -th attention head, respectively.  $H$  represents the number of attention heads, and  $\| \cdot \|$  denotes the concatenation of the  $H$  vectors. The softmax function  $\delta(\cdot)$  is applied. In our self-attention layer, the embedding  $\mathbf{e}_i$  captures the pairwise interactions between region  $r_i$  and  $r_j$  with respect to the region-wise POI semantics.

### 2.3 Heterogeneous Spatial-Temporal GNNs

We model our data as a spatial-temporal graph  $\mathcal{G}$ , which is composed of three matrices, namely region POI matrix  $\mathbf{P}$ , human trajectory matrix  $\mathbf{M}$  and spatial distance matrix  $\mathcal{D}$ . Thus the relations of the nodes in graph  $\mathcal{G}$  are diverse and can be classified into five types, namely relations  $\mathcal{R}_p$  based on POI similarities of regions, relations  $\mathcal{R}_m$  based on urban flow between regions, relations  $\mathcal{R}_d$  based on distances of regions, relations  $\mathcal{R}_{pm}$  between the POI subgraph and the mobility subgraph, and relations  $\mathcal{R}_{md}$  between the mobility subgraph and spatial distance graph. And the relation set  $\mathcal{R}$  is shown as  $\mathcal{R} = \{\mathcal{R}_p, \mathcal{R}_m, \mathcal{R}_d, \mathcal{R}_{pm}, \mathcal{R}_{md}\}$ . To handle the heterogeneous relationship, we design the relation-aware message passing paradigm as follows:

$$\mathbf{h}_i^{(l+1)} = \sigma \left( \sum_{\gamma \in \mathcal{R}} \sum_{j \in \mathcal{N}_i^\gamma} \alpha_{i,\gamma} \mathbf{W}_\gamma^{(l)} \mathbf{h}_j^{(l)} \right); \quad \alpha_{i,\gamma} = \frac{1}{|\mathcal{N}_i^\gamma|} \quad (2)$$

where  $\mathcal{N}_i^\gamma$  denotes neighbour set of region  $r_i$  via relation  $\gamma$ .  $\mathcal{R}$  is the relation set.  $\mathbf{h}_i^{(l+1)}, \mathbf{h}_j^{(l)} \in \mathbb{R}^d$  represents the hidden embedding vectors of the  $i$ -th region vertex in the  $(l+1)$ -th graph layer and the  $j$ -th region vertex in the  $l$ -th graph neural layer, respectively.  $\sigma(\cdot)$  denotes the ReLU activation function.  $\alpha_{i,\gamma} \in \mathbb{R}$  represents the normalization weight of region vertex pair  $(r_i, r_j)$ , which is calculated using the degrees of the vertices.  $\mathbf{W}_\gamma^{(l)} \in \mathbb{R}^{d \times d}$  presents the learning weights for the  $l$ -th layer. HGAurban combines the multi-order embeddings to fully utilize the data obtained from the

multi-hop neighborhood. The cross-view message passing mechanism is shown in the following formula:

$$\mathbf{H} = \sum_{l=0}^L \mathbf{H}^{(l)}; \quad \mathbf{H}^{(l+1)} = \sigma(\mathbf{D}^{-\frac{1}{2}} \mathbf{A} \mathbf{D}^{-\frac{1}{2}} \mathbf{H}^{(l)} \mathbf{W}_Y^{(l+1)\top}) \quad (3)$$

where  $\mathbf{H} \in \mathbb{R}^{|\mathcal{V}| \times d}$  is the embedding matrix, whose rows are regional embedding vectors  $\mathbf{h}_i$ .  $L$  is the number of the model layers.  $\mathbf{A} \in \mathbb{R}^{|\mathcal{V}| \times |\mathcal{V}|}$  denotes the adjacent matrix with self-loop. The diagonal degree matrix is denoted as  $\mathbf{D} \in \mathbb{R}^{|\mathcal{V}| \times |\mathcal{V}|}$ .

### 2.4 The Layout of Spatial-Temporal Graph Mask Autoencoder

Given the spatial-temporal graph  $\mathcal{G}$ , the encoder function  $f_E$  and the decoder function  $f_D$ , Graph mask autoencoder (GMAE) aims to reconstruct the spatial-temporal graph  $\mathcal{G}'$  as follows:

$$\mathbf{H} = f_E(\tilde{\mathbf{A}}, \tilde{\mathbf{X}}), \quad \mathcal{G}' = f_D(\tilde{\mathbf{A}}', \tilde{\mathbf{H}}) \quad (4)$$

where  $\tilde{\mathbf{A}}$  and  $\tilde{\mathbf{X}}$  denote the masked adjacent matrix and mask node embedding matrix respectively. And  $\tilde{\mathbf{A}}'$  and  $\tilde{\mathbf{H}}$  represent the re-masked adjacent matrix and the re-masked node embedding matrix respectively. Details of GMAE design for the spatial-temporal graph  $\mathcal{G}$  are in the following sections.

**2.4.1 Motivation of Features and Structure Reconstruction.** The primary motivation behind reconstructing features and structure in GAE lies in the versatility they offer to address different tasks and applications. In certain scenarios, an effective representation of the graph's structure  $\mathbf{A}$  and node features  $\mathbf{X}$  can then be utilized for tasks like link prediction or node classification. This can be formulated with coefficient  $\alpha$  and activation  $\sigma$  as follows:

$$\underbrace{\mathcal{L}}_{\text{Graph}} = \underbrace{\|\mathbf{X} - \hat{\mathbf{X}}\|_F^2}_{\text{Node}} + \alpha \cdot \underbrace{\|\mathbf{A} - \sigma(\mathbf{H} \cdot \mathbf{H}^\top)\|_F^2}_{\text{Structure}} \quad (5)$$

However, GAE often prioritizes reconstructing the features  $\mathbf{X}$  while minimizing or ignoring the reconstruction error related to the structure  $\mathbf{A}$ . Actually, by adapting  $\alpha$  based on the specific task and application, GAEs can effectively learn representations that cater to the demands of diverse graph-based problems. Inspired by recent studies [22, 26] and the significance of different types in our heterogeneous graph, we propose to reconstruct both the structure and features in our HGAurban. Besides, we use a mask mechanism-based generative self-supervised learning paradigm, which allows

for effective learning of the spatial-temporal dependencies of region-wise within the graph.

Jointly reconstructing both the structure and features offers several key advantages: **(1) Enhanced graph representation.** The model can achieve superior graph representation learning and node classification, which is particularly crucial for graphs with multiple relations. **(2) Improved relationship nuance capture.** It can effectively capture the subtleties of the relationships between nodes, resulting in a more accurate representation of the graph structure. Such a detailed representation is challenging to achieve due to the complexity and multifaceted nature of node relationships.

**2.4.2 Reconstructing Features and Structures using Mask Mechanism.** Developing effective feature-oriented Graph Autoencoders (GAEs) is challenging due to the limited node feature dimensionality in graphs. Existing GAEs, primarily focused on feature reconstruction, often neglect the risk of learning the "identity function" when the hidden vector dimension surpasses the input, rendering the learned representation useless. To address this issue, we propose the utilization of denoising autoencoders, which intentionally introduce corruption to the input data. Masked autoencoders have demonstrated success in computer vision (CV) and natural language processing (NLP) tasks, where masking is employed as a corruption mechanism. In our suggested approach for GAEs, we advocate for the incorporation of masked autoencoders. Specifically, we randomly select a subset of nodes denoted as  $\tilde{\mathcal{V}} \in \mathcal{V}$  and mask their node features by utilizing a learned vector  $x_M \in \mathbb{R}^d$ . This strategy aims to prevent GAEs from learning the 'identity function' and enhances the quality of the learned embeddings. By integrating masked autoencoders, we effectively address the challenge of feature reconstruction in GAEs and pave the way for more efficient and meaningful learning of feature-oriented graph representations. The masking process can be defined using Eq. 6:

$$x_i = \begin{cases} x_M, & \text{if } v_i \in \tilde{\mathcal{V}} \\ x_i, & \text{if } v_i \notin \tilde{\mathcal{V}} \end{cases} \quad (6)$$

Given the masked node feature matrix  $\tilde{\mathbf{X}}$ , one of the objectives of HGAurban is to reconstruct masked node features of regions (e.g.,  $r_i$ ) in  $\tilde{\mathcal{V}}$  and masked the adjacent matrix  $\tilde{\mathbf{A}}$  via a learned vector  $a_M$ . In GNNs, the hidden embedding vector of each node is affected by its neighboring nodes' embedding vectors according to the message passing mechanism. However, selecting nodes via scores can lead to bias, for example, if all neighbors of one node are selected or masked. To prevent bias in node selection, random node selection or sampling is taken into account the entire graph structure rather than just local node properties, which also improves robustness.

**2.4.3 Remask Decoder via GNNs.** The role of the decoder function  $f_D$  is to map the hidden embedding vectors  $\tilde{\mathbf{H}}$  to the input graph  $\mathcal{G}'$  and its node embedding matrix  $\mathbf{X}'$ , based on the semantic level of the target input graph  $\mathcal{G}$  and its corresponding node embedding matrix  $\mathbf{X}$  [9]. For example, in NLP, an MLP is typically sufficient for targets of one-hot missing words with rich semantics, as there is no structure semantics to consider. However, in CV, a transformer is often used as the decoder to recover pixel spots with few semantics.

To better capture graph structure information, we adopt GCN as the decoder in our method. This is in contrast to traditional GAEs

that typically utilize an MLP to decode the hidden embedding matrix, which results in a similar output to the input graph embedding matrix. Using an MLP as the decoder cannot capture the structure semantics of graphs, so we choose GCN to better capture this.

To further improve the ability of the encoder to learn compressed graph representations, we adopt a remask mechanism in the decoder, inspired by [10]. The process is represented as following:

$$\tilde{h}_i = \begin{cases} h_M & v_i \in \tilde{\mathcal{V}} \\ h_i & v_i \notin \tilde{\mathcal{V}} \end{cases} \quad (7)$$

Here,  $\tilde{\mathbf{H}} = \text{REMASK}(\mathbf{H})$ , where a masked node is forced to build its input feature based on the neighboring non-masked nodes' hidden embedding vectors, under the guidance of the GCN decoder. This approach helps ensure that the learned embeddings are both informative and compressed, which can improve the overall region representation ability of our framework HGAurban.

## 2.5 Model Optimization and Complexity

To optimize our method HGAurban, we adopt the cosine similarity loss, denoted as  $\mathcal{L}_1$ , to optimize remasked node features and initial input node features. Besides, to help optimize structure masking, another loss MSE is adopted. These two losses are shown as:

$$\begin{aligned} \mathcal{L}_1 &= \frac{1}{N} \sum_{i=1}^N \left( 1 - \frac{h_i^T \tilde{h}_i}{\|h_i\| \cdot \|\tilde{h}_i\|} \right); \\ \mathcal{L}_2 &= \|\mathbf{E} - \sigma(\tilde{\mathbf{A}}' \cdot \tilde{\mathbf{A}}'^T)\|_2^2 \end{aligned} \quad (8)$$

where  $\mathbf{E}$  is the hidden matrix of initial adjacent matrix  $\mathbf{A}$ .

By leveraging generative self-supervised learning tasks during pretraining, our proposed framework, HGAurban, aims to produce high-quality region embeddings. The optimization goal of our framework HGAurban can be formalized as follows:

$$\min_{\theta} \mathcal{L}_{rec}(\mathbf{A}, \mathbf{X}, \tilde{\mathbf{A}}', \tilde{\mathbf{X}}'), \quad \mathcal{L}_{rec} = \mathcal{L}_1 + \mathcal{L}_2 \quad (9)$$

where  $\theta$  denotes the parameters of the model,  $\mathcal{L}_{rec}$  is the reconstruction loss that measures the difference between the original and reconstructed adjacency matrix  $\mathbf{A}$  and node feature matrix  $\mathbf{X}$ . The objective function ensures that the model can accurately reconstruct both the graph structure and node features, while the second term encourages the model to learn representations that are useful for predicting node features in a self-supervised manner. Overall, the optimization goal of our framework reflects our aim to learn high-quality region embeddings that can be used for downstream tasks such as node classification, link prediction, and community detection. And the time complexity of our framework HGAurban is divided into two parts: first of all, the multi-view space-time message passing paradigm has a complexity of  $\mathcal{O}(|\mathcal{V}| \times L \times d)$ , where  $N$  and  $L$  denote the number of edges and graph propagation layers, respectively. Secondly, for loss calculation, HGAurban takes  $\mathcal{O}(S \times |\tilde{\mathcal{V}}| \times d)$ , where  $S$  denotes the number of sampled nodes included in each batch for the spatial-temporal graph.

## 2.6 In-depth Theory Analysis of HGAurban

In this section, we aim to provide in-depth analysis of our framework HGAurban. We present a small HGAurban loss denoting a small spatial-temporal alignment loss. Firstly, we have the following

**Algorithm 1:** HGAurban: Heterogeneous Graph Autoencoding for Urban Spatial-Temporal Learning**Require:**

- 1: Spatio-temporal graph  $\mathcal{G} = (\mathcal{V}, \mathcal{E})$  with:
- 2: POI matrix  $\mathcal{P} \in \mathbb{R}^{I \times C}$
- 3: Mobility matrix  $\mathbf{M} \in \mathbb{R}^{I \times I \times T}$
- 4: Distance matrix  $\mathcal{D} \in \mathbb{R}^{I \times I}$
- 5: Mask ratio  $p_{\text{mask}} \in (0, 1)$
- 6: Relation set  $\mathcal{R} = \{\mathcal{R}_p, \mathcal{R}_m, \mathcal{R}_d, \mathcal{R}_{pm}, \mathcal{R}_{md}\}$

**Ensure:** Reconstructed adjacency  $\hat{\mathbf{A}}$  and features  $\hat{\mathbf{X}}$ 

- 7: /\* **Graph Partitioning** \*/
- 8: Divide urban area into  $I$  regions  $\{r_i\}_{i=1}^I$
- 9: Initialize node features  $\mathbf{X} \leftarrow \text{Concat}(\mathbf{P}, \mathbf{M}, \mathcal{D})$
- 10: /\* **Masked Autoencoder Setup** \*/
- 11: Randomly select  $\mathcal{V}_{\text{mask}} \subset \mathcal{V}$  with  $|\mathcal{V}_{\text{mask}}| = p_{\text{mask}}|\mathcal{V}|$
- 12: Generate masked graph  $\tilde{\mathcal{G}}$  via Eq. 6 and Eq. 7
- 13: /\* **Encoder: Heterogeneous GNN** \*/
- 14: **for**  $l = 1$  **to**  $L$  **do**
- 15: Multi-relational message passing:
- 16:  $\mathbf{h}_i^{(l+1)} \leftarrow \sigma\left(\sum_{\gamma \in \mathcal{R}} \sum_{j \in \mathcal{N}_i^\gamma} \frac{1}{|\mathcal{N}_i^\gamma|} \mathbf{W}_\gamma^{(l)} \mathbf{h}_j^{(l)}\right)$
- 17: **end for**
- 18:  $\mathbf{H} \leftarrow \sum_{l=0}^L \mathbf{H}^{(l)}$  {Final embeddings}
- 19: /\* **Decoder: Reconstruction** \*/
- 20: Remask embeddings  $\tilde{\mathbf{H}} \leftarrow \text{REMASK}(\mathbf{H})$  (Eq. 7)
- 21:  $\hat{\mathbf{X}} \leftarrow \text{GCN-Decoder}(\tilde{\mathbf{H}})$
- 22:  $\hat{\mathbf{A}} \leftarrow \sigma(\mathbf{H}\mathbf{H}^\top)$
- 23: /\* **Loss Computation** \*/
- 24: Feature loss:  $\mathcal{L}_1 \leftarrow \frac{1}{N} \sum_{i=1}^N \left(1 - \cos(\mathbf{h}_i, \tilde{\mathbf{h}}_i)\right)$
- 25: Structure loss:  $\mathcal{L}_2 \leftarrow \|\mathbf{A} - \sigma(\hat{\mathbf{A}}\hat{\mathbf{A}}^\top)\|_F^2$
- 26: Total loss:  $\mathcal{L} \leftarrow \mathcal{L}_1 + \mathcal{L}_2$
- 27: **return**  $\hat{\mathbf{A}}, \hat{\mathbf{X}}$

assumption: There exists a pseudo-inverse encoder  $f_E$  which also the resulting pseudo autoencoder  $s_g = \{g, f_g\}$  satisfies  $\mathbb{E}\|s_g(z) - z\| \leq \epsilon$ , where  $z$  denotes masked representation of the input graph  $\mathcal{G}$ . Following this assumption, our method performs input-output alignment on the masked spatial-temporal graph. The lower bound of  $\mathcal{L}_{\text{rec}} \geq \mathcal{L}_{\text{asym}} - \epsilon + C$ , where  $C$  is a constant number and  $\mathcal{L}_{\text{asym}}$  is presented as following for the spatial-temporal graph  $\mathcal{G}$ :

$$\mathcal{L}_{\text{asym}} = -\mathbf{E}_{x_1, x_2} f(x_1) s_g(x_2) = -\text{tr}(\mathbf{H}_g^T \tilde{\mathbf{A}}_m \mathbf{H}) \quad (10)$$

where  $\mathbf{H}$  is the output matrix of our method HGAurban on  $\mathcal{G}_1$  whose  $x_1$ -row is  $\mathbf{H}_{x_1} = \sqrt{d_{x_1}} f(x_1)$ , and  $\mathbf{H}_g$  is the output matrix of  $s_g$  on  $\mathcal{G}_2$  whose  $x_2$ -th row is  $(\mathbf{H}_g)_{x_2} = \sqrt{d_{x_2}} s_g(x_2)$ . Thus, a small HGAurban loss implies a small alignment loss as a lower bound, which also verifies align mask and unmask view via HGAurban. This again verifies that our method can obtain the same level performance as the contrastive learning loss without data augmentation.

### 3 EXPERIMENTS

We conduct experiments to answer the following questions: **RQ1:** How does the HGAurban fare in terms of different baselines across multiple spatial-temporal learning applications including traffic prediction, crime prediction and house price prediction? **RQ2:** How

**Table 1: Data Description of Experimented Datasets**

Data	Description of Chicago Data	Description of NYC data
Census	Boundaries of 234 regions split by streets in a certain district, Chicago	Boundaries of 180 regions split by streets in Manhattan, New York
Taxi trips	Total 386,272 taxi trips during a month	Total 1,445,285 taxi trips during a month
Crime data	Total 321,876 crime records during 1 year	Total 108,575 crime records during 1 year
POI data	Total 3,680,125 POI locations of 130 categories	Total 20,569 POI locations of 50 categories
House price	Total 44,447 house price data in a certain district, Chicago	Total 22,540 house price data in Manhattan, New York

do various data perspectives and generative elements impact the effectiveness of region representation? **RQ3:** How well does our HGAurban fare in representation learning over areas with various levels of data sparsity? **RQ4:** What effects do different hyperparameter settings have on the performance of the HGAurban's region representation? **RQ5:** How the efficiency of our method HGAurban than other region representation methods?

### 3.1 Experimental Setup

**3.1.1 Datasets and Protocols.** With the aim of assessing the effectiveness of our HGAurban framework, we gathered real-world datasets from two major cities, namely Chicago and New York City. These datasets were utilized to perform three spatio-temporal mining tasks: crime prediction and traffic flow forecasting, as well as property price prediction. To ensure a comprehensive evaluation, we included various types of crimes in our datasets. For the Chicago database, crimes such as Theft, Battery, Assault, and Damage were considered, while the NYC database encompassed crimes such as Burglary, Larceny, Robbery, and Assault. The selection of crime types aligns with the parameters in [35]. A detailed description of the data is shown in Table 1.

**3.1.2 Hyperparameter Settings.** Following existing region representation studies [34, 38], we set the dimensionality  $d$  as 96. And from the hyperparameter study experiments, we find that the framework HGAurban obtains the best performance when the GCN depth is set as 2. And the learning rate is 0.001 with weight decay 0.0005. For crime prediction backbone model, the learning rate of ST-SHN is set as 0.001 and weight decay is 0.96. The depth of the spatial aggregation layer is set as 2. For traffic prediction backbone model ST-GCN, the input length is 12 time intervals with each interval setting as 5 minutes. And the output is 15 minutes' results of traffic flow prediction.

**3.1.3 Implementation Details.** To be fair, we implement HGAurban and other baselines in Python 3.8, pytorch 1.7.0 with cuda 11.3 for our method implementation and tensorflow 1.15.3 for traffic prediction and crime prediction. The experiments are conducted on a server with 10-cores of Intel(R) Core(TM) i9-9820X CPU @ 3.30GHz 64.0GB RAM and one Nvidia GeForce RTX 3090 GPU.

**3.1.4 Baselines.** We use 15 baselines from three research lines namely, graph representation approaches, graph contrastive learning models, and spatial-temporal region representation methods for comparison in order to thoroughly assess our HGAurban model.

#### Graph Representation Approaches:

- **Node2vec** [7] encodes graph structural data using a random walk-based skip-gram.

**Table 2: Overall performance in crime forecasting, traffic prediction, and house price prediction.**

Model	Crime Prediction				Traffic Prediction						House Price Prediction			
	CHI-Crime		NYC-Crime		CHI-Taxi		NYC-Bike		NYC-Taxi		CHI-House		NYC-House	
	MAE ↓	MAPE ↓	MAE ↓	MAPE ↓	MAE ↓	RMSE ↓	MAE ↓	RMSE ↓	MAE ↓	RMSE ↓	MAE ↓	MAPE ↓	MAE ↓	MAPE ↓
ST-SHN	2.0259	0.9987	4.4004	0.9861	–	–	–	–	–	–	–	–	–	–
ST-GCN	–	–	–	–	0.1395	0.5933	0.9240	1.8562	1.4093	4.1766	–	–	–	–
Node2vec	1.6334	0.8605	4.3646	0.9454	0.1206	0.5803	0.9093	1.8513	1.3508	4.0105	13137.2178	44.4278	4832.6905	19.8942
GCN	1.6061	0.8546	4.3257	0.9234	0.1174	0.5707	0.9144	1.8321	1.3819	4.0200	13074.2121	42.6572	4840.7394	18.3315
GAT	1.5742	0.8830	4.3455	0.9267	0.1105	0.5712	0.9110	1.8466	1.3746	4.0153	13024.7843	43.3221	4799.8482	18.3433
GraphSage	1.5960	0.8713	4.3080	0.9255	0.1196	0.5796	0.9102	1.8473	1.3966	4.0801	13145.5623	44.3167	4875.6026	18.4570
GAE	1.5711	0.8801	4.3749	0.9343	0.1103	0.5701	0.9132	1.8412	1.3719	4.0337	13278.3256	42.3221	4896.9564	18.3114
GraphCL	1.2332	0.6293	3.3075	0.6771	0.0812	0.5364	0.8582	1.8180	1.3022	3.7029	10752.5693	28.8374	4562.7279	11.3055
RGCL	1.1946	0.6081	3.1026	0.6323	0.0797	0.5052	0.8319	1.8107	1.2973	3.6865	10673.3289	27.5279	4439.0733	10.2375
POI	1.3047	0.8142	4.0069	0.8658	0.0933	0.5578	0.8892	1.8277	1.3316	3.9872	12045.3212	33.5049	4703.3755	16.7920
HDGE	1.3586	0.8273	4.2021	0.7821	0.0865	0.5502	0.8667	1.8251	1.2997	3.9846	11976.3215	30.8451	4677.6905	12.5192
ZE-Mob	1.3954	0.8249	4.3560	0.8012	0.1002	0.5668	0.8900	1.8359	1.3314	4.0366	12351.1321	38.6171	4730.6927	16.2586
MV-PN	1.3370	0.8132	4.2342	0.7791	0.0903	0.5502	0.8886	1.8313	1.3306	3.9530	12565.0607	39.7812	4798.2951	17.0418
CGAL	1.3386	0.7950	4.1782	0.7506	0.1013	0.5682	0.9097	1.8557	1.3353	4.0671	12094.5869	36.9078	4731.8159	16.5454
MVURE	1.2586	0.7087	3.7683	0.7318	0.0874	0.5405	0.8699	1.8157	1.3007	3.6715	11095.5323	34.8954	4675.1626	15.9860
AutoST	1.0480	0.4787	2.1073	0.5241	0.0665	0.4931	0.8364	1.8145	1.2871	3.6446	10463.7715	25.7575	4517.7276	7.1660
MGFN	1.2538	0.6937	3.5971	0.7065	0.0831	0.5385	0.8783	1.8163	1.3266	3.7514	10792.7834	29.9832	4651.3451	12.9752
<b>HGAurban</b>	<b>1.0438</b>	<b>0.4608</b>	<b>2.1060</b>	<b>0.5203</b>	<b>0.0606</b>	<b>0.4817</b>	<b>0.7787</b>	<b>1.8079</b>	<b>1.2778</b>	<b>3.6335</b>	<b>10375.9982</b>	<b>23.1751</b>	<b>4432.1934</b>	<b>6.8785</b>
P-Value	5.27e-12	1.74e-14	2.7e-13	8.22e-11	1.32e-6	7.34e-10	2.13e-10	9.38e-4	1.24e-18	5.37e-21	2.18e-5	1.78e-4	1.91e-4	2.75e-4

- **GCN** [15] carries out the convolution-based message transfer along the edges between neighboring nodes for refinement.
- **GraphSage** [8] is a graph neural architecture that permits the accumulation of information from the sub-graph structures.
- **GAE** [14] maps node into latent embedding space by the Graph Auto-encoder using the input reconstruction objective.
- **GAT** [28] varies the degrees of significance among nearby nodes, and improves GNNs' capacity to discriminate between diverse inputs. To optimize the performance of GNN-based approaches, the number of information propagation layers is adjusted from a range of {1,2,3,4}.

#### Graph Contrastive Learning Models:

- **GraphCL** [37] is based on the maximizing of mutual knowledge and generates many contrastive viewpoints for augmentation.
- **RGCL** [17] have been fine-tuned to manage the contrastive augmentation in order to allow for fair comparison.

#### Spatial-Temporal Region Representation Methods:

- **POI** [24] uses TF-IDF tokenization with the provided POI matrix and the POI properties to represent spatial regions.
- **HDGE** [30] creates a crowd flow graph using human trajectory data and embeds regions into latent vectors to protect the structural data of the network and capture mobility patterns.
- **ZE-Mob** [36] uses region correlations to create embeddings while taking into account human movement and taxi moving traces based on multi-view data sources.
- **MV-PN** [5] models intra-regional and inter-regional correlations with an encoder-decoder network.
- **CGAL** [48] is a technique for graph-regularized adversarial learning that uses pairwise graph relationships to embed regions in latent space via the graph attention neural network.
- **MVURE** [38] makes use of the graph attention mechanism to simulate region correlations with the built-in properties of the region and data on human mobility.
- **AutoST** [40] is a method that utilizes contrastive self-supervised learning method via multi-view graph to model region representation learning problem on traffic and crime prediction tasks.

- **MGFN** [34] aggregates information for both intra-pattern and inter-pattern patterns, and encodes region embeddings with multi-level cross-attention without region function information.

### 3.2 Effectiveness Evaluation (RQ1)

Table 2 shows a performance comparison of all methods on three tasks (crime prediction, traffic prediction, and house price prediction) in terms of MAE, MAPE, and RMSE.

**Crime prediction.** We show crime prediction results in Table 2. From Table 2, we summarize observations as follows:

- On both datasets, our framework HGAurban performs best at predicting crimes, indicating the viability of our generative spatio-temporal graph self-supervised learning approach. In specific, we attribute the benefits to: i) HGAurban can capture both the multi-view area relationships from multi-typed data sources (i.e., POI semantics, human motion traces, geographical coordinates) thanks to masking different types of relations. ii) The adaptive data augmentation way of HGAurban via the mask mechanism on nodes and relations improves the representation ability against noise disturbance and skewed data distribution.
- While existing approaches for region representation (such as CGAL, MVURE, and MGFN) aim to capture the mobility-based region correlations, they are susceptible to noisy edges in their built mobility-based region graphs. The performance of region representation learning will be hampered by the propagation of information propagation between less-relevant regions. Besides, the spatial dependence modeling in such baselines is constrained by the skewed distribution of mobility data. Our HGAurban which is complementary to the mobility-based region connections, adds region self-discrimination supervision signals to the region embedding paradigm to solve these limitations.
- The large enhancement of HGAurban over the compared graph embedding techniques (i.e., GCN and GAT) further supports the significance of generative self-supervised learning paradigm. When a message passes over the edges of a task-irrelevant region in the graph neural paradigm, noise effects will be enhanced. The information compiled from all the nearby mobility-based or

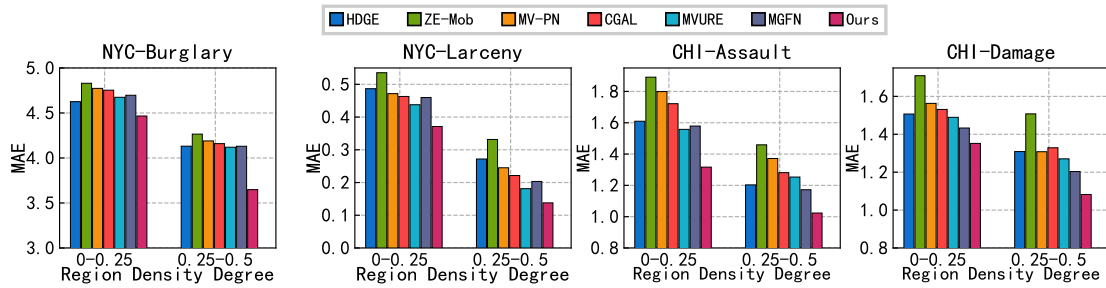


Figure 2: Results on NYC and CHI crime for four crime types *w.r.t* different data density degrees.

POI-based graph regions may be misleading when it comes to encoding the actual underlying crime trends.

**Traffic prediction.** We present traffic prediction results in Table 2 with the following observations:

- The significance of the generative self-supervised learning with the mask mechanism is further supported by the significant performance improvement of HGAUrban over the compared graph embedding techniques (such as GCN, GAT, and GAE). In the graph neural paradigm, noise effects will be amplified when messages crosses edges of regions that are unrelated to the task.
- To find traffic patterns or mine human behavior, region representation methods (*i.e.*, MVURE, MGFN) need enough data, which means they cannot handle long-tail data. Contrarily, contrastive learning with masking nodes or links mechanism has better skewed data distribution adaption.

### 3.3 Ablation Study (RQ2)

To evaluate the effectiveness of each component of our framework HGAUrban, we perform an ablation study and present results *w.r.t* traffic prediction and crime prediction in Figure 4 and Figure 5. Particularly, we conduct an ablation study several variants including “RP GCN” by replacing GCN with MLP, “w/o Structure Mask”, “w/o Node Mask”, and “w/o Edge Type Mask” by removing masking links or masking nodes.

**Analysis on Crime prediction.** The figure demonstrates the impact of different components on region representation for crime prediction. “RP GCN” replacing GCN with a 2-layer MLP, contributes the most to performance improvement compared to “w/o Structure Mask”, “w/o Edge Type Mask”, and “w/o Node Mask” GCN captures spatial-temporal graph structure semantics, unlike MLP. “w/o Node Mask” has a larger impact than “w/o Structure Mask” as masking nodes directly affects region representations. Masking different link types positively affects region representations, emphasizing the significance of masking links in the heterogeneous graph. “w/o Edge Type Mask” which doesn’t mask edges, shows a notable performance decline, highlighting the effectiveness of edge type masking in our HGAUrban model. Overall, integrating GCN, node masking, and edge-type masking enhances the performance of our HGAUrban framework.

**Analysis on Traffic prediction.** Based on Figure 4, GCN has the greatest impact on improving region representations and traffic prediction, especially for longer time horizons. Masking edge types significantly improves traffic flow prediction accuracy. Masking nodes

Table 3: Overall Performance Comparison in Traffic Prediction Improvement

Methods	NYC-Taxi		Methods	NYC-Taxi	
	MAE	RMSE		MAE	RMSE
GMAN	2.0812	3.0215	STGCN	1.4093	4.1766
w/MVURE	1.8795	2.8337	w/MVURE	1.3007	3.6715
w/MGFN	1.9261	2.8337	w/MGFN	1.3266	3.7514
w/HGAUrban	1.8403	2.7032	w/HGAUrban	1.2415	3.6375

and graph structure also contribute positively by refining region representations and capturing spatial relationships. Incorporating POI information enhances region representations and enables the encoding of different region relations. Overall, the combination of GCN, edge type masking, node masking, and POI integration contributes to the success of our HGAUrban method in learning region representations and achieving accurate traffic predictions.

### 3.4 More Effectiveness Evaluation Results (RQ1)

Results for the data on home prices in Chicago and New York City are shown in Table 2 and more analysis details are below. A Lasso regression approach uses the input embeddings from the learned region representations created using various methods.

- HGAUrban consistently performs at the highest level. On the other hand, MVURE and MGFN perform better when using data from the housing markets of New York and Chicago, respectively. This is because they mine human patterns, which connect comparable or nearby places. We also notice that the POI technique performs well because it creates connections between POIs of regions and core shopping regions, which include POIs that are distinct from those in remote towns.
- Methods taking advantage of region representations outperform those using network embeddings in terms of performance. The basis for this investigation is that region-wise dependencies from both the spatial and temporal dimensions cannot be effectively encoded by conventional graph-based approaches (such as GCN).
- Table 3 shows results of improvement of existing widely used traffic prediction methods (*e.g.*, GMAN, STGCN) based on several region representation baselines and our method HGAUrban. The superior performance further validates the effectiveness of generative self-supervised learning with a masking mechanism for denoising data. In contrast, methods like MVURE and MGFN require significantly more data to uncover human patterns.

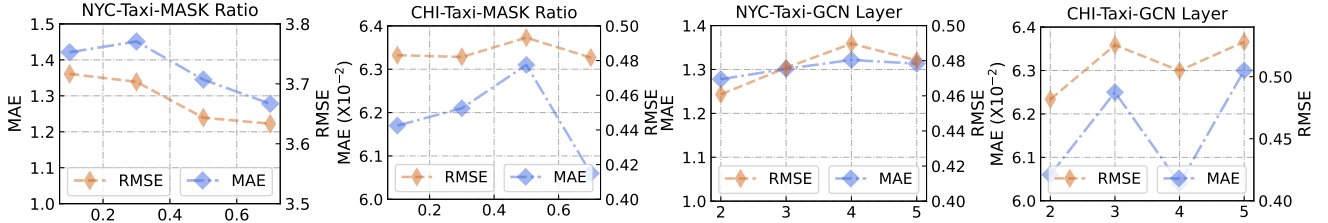


Figure 3: Hyperparameter study on traffic prediction

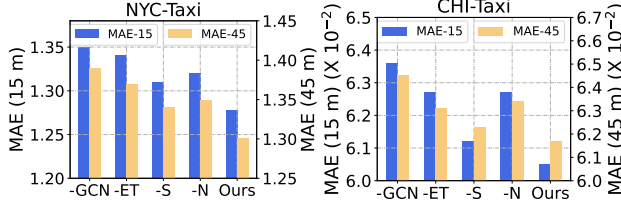


Figure 4: Ablation study of HGAUrban on traffic prediction

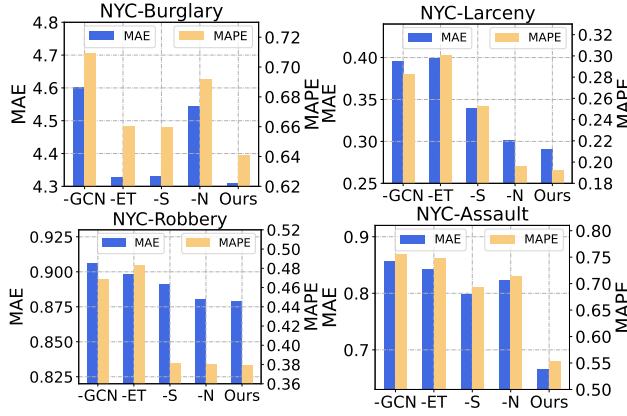


Figure 5: Ablation study of HGAUrban on crime prediction

### 3.5 Model Robustness Study (RQ3)

We also conduct experiments to test how well our framework HGAUrban stands up to data sparsity. To accomplish this, we assess the forecast accuracy of regions with various densities independently. Here, the ratio of non-zero elements (crime occurs) in the region-specific crime occurrence sequence  $Z_r$  is used to estimate the density degree of each region. We divide sparse areas with a crime density degree of less than 0.5 into two groups, (0.0, 0.25] and (0.25, 0.5] specifically. Figure 2 presents the evaluation findings. We see that our HGAUrban constantly performs better than alternative approaches. Thus, this experiment once more indicates how masking mechanism on nodes and the structure for self-supervised learning into the spatial-temporal region representation learning provides very accurate and reliable crime prediction in all scenarios with varying crime density degrees. To mine human behaviors or movement patterns, existing region representation algorithms (such MVURE and MGFN) require a huge quantity of data, which results in lower performance on the sparse data. Another finding acknowledges that typical graph learning techniques now in use (such as GNN-based approaches including GCN) are unable to efficiently build high-quality representations of regions with sparse crime data via the spatial-temporal graph.

The second line of Figure 2 present more details about the evaluation findings of the model robustness. We see that HGAUrban constantly performs better than alternative approaches. Thus, this experiment once more indicates how masking mechanism on nodes and the structure for self-supervised learning into the spatial-temporal region representation learning provides very accurate and reliable crime prediction in all scenarios with varying crime density degrees. To mine human behaviors or movement patterns, existing region representation algorithms (MVURE and MGFN) require a huge quantity of data, which results in lower performance on the sparse data. Another finding acknowledges that typical graph learning techniques now in use (*i.e.*, GNN-based approaches like CGN) are unable to efficiently build high-quality representations of regions with sparse crime data via the spatial-temporal graph.

### 3.6 Hyperparameter Study (RQ4)

We conduct the hyperparameter study on the parameters including the mask ratio of nodes and links with the range [0.1, 0.3, 0.5, 0.7], and the number of CGN layer from the range [2, 3, 4, 5] on crime prediction task and traffic prediction *w.r.t* New York and Chicago in terms of MAE, MAPE and RMSE. We provide results in Figure 3. From figures, we can have the following observations: (1) For the impact of mask ratio of nodes and structure, we find that the model HGAUrban can achieve the best performance on crime prediction and traffic prediction on all datasets when the mask ratio of nodes and links is set as 0.7. And the performance decreases with the decrease of mask ratio. This verifies that masking nodes and links do not always bring better model representation ability. Smaller mask ratios (*e.g.*, [0.1, 0.3, 0.5]) may not denoise noisy nodes and links completely, which leads to bad performance. (2) For the effect of the number of GCN layer, we find that our framework HGAUrban achieves the best performance when the number of GCN layer is set as 2. We notice that the performance decreases with the increasing number of GCN layer. This may be caused by over-smoothing issue on region representation with the increasing number of the GCN layer. (3) We also investigate the consuming time of our model HGAUrban with varied hyperparameters. We observe that time cost increases with increasing mask ratio of nodes and links, since our model HGAUrban requires to reconstruct more nodes' representation and new links when masking more nodes and links. Similarity, time consuming is larger when the more layers of GCN due to that the message passing between GCN layers need more time.

### 3.7 Model Efficiency Study (RQ5)

We investigate the efficiency of our method HGAUrban and existing region representation learning methods *w.r.t* training time. We provide results in Table 4. All of these methods are adopted in

**Table 4: Computational cost (seconds) of our HGAurban and SOTA spatial-temporal region representation methods. MAE and MAPE are estimated for NYC crime prediction results.**

Models	HDGE	ZE-Mob	MV-PN	CGAL	MVURE	MGFN	Ours
Training	303.7	82.7	33.4	4144.8	240.7	852.3	124.5
MAE	4.2021	4.3560	4.2342	4.1782	3.7683	3.5971	2.1060
MAPE	0.7821	0.8012	0.7791	0.7506	0.7318	0.7065	0.5203

python 3.8, pytorch 1.7.0 with cuda 11.3 and tensorflow 1.15.3 (GPU version). The experiments are conducted in the same server. From the table, By comparing the model efficiency of HGAurban to the baselines (e.g., HDGE, MVURE and MGFN), we can see that it is competitive, indicating that it has the capacity to handle massive amounts of spatial-temporal data. The performance of the region representation is greatly improved by the generative self-supervised learning paradigms while incurring little additional expense.

## 4 RELATED WORK

**Self-supervised Learning for Spatial-Temporal Graphs.** In the domain of self-supervised learning (SSL) for spatial-temporal graphs, a line of research has emerged, focusing on graph-based SSL methods specifically designed for capturing the spatial and temporal dependencies within the graph structure. Several recent studies have contributed to this area, including [11, 18, 40, 41], and [12]. Liu et al. [18] propose an innovative approach that adopts the self-supervised learning paradigm to leverage supplementary information that is typically inaccessible due to privacy concerns. Ji et al. [11] introduce self-supervised learning paradigms in a spatial-temporal traffic prediction framework. The proposed method enhances the traffic pattern representations to capture both spatial and temporal heterogeneity within the spatial-temporal graph, leading to improved traffic prediction performance. Overall, these studies demonstrate the effectiveness of methods of self-supervised learning in capturing spatial and temporal dependencies within spatial-temporal graphs. By leveraging additional information or incorporating self-supervised learning paradigms, these approaches enhance representation learning and improve the performance of downstream tasks in various domains, including POI recommendation, traffic prediction, and region representations on the spatial-temporal graph for downstream tasks.

**Graph Mask Autoencoder.** Graph autoencoder methods have emerged as a category of generative self-supervised learning approaches that aim to construct input graphs directly, eliminating the need for high-quality data augmentation typically required in contrastive self-supervised learning. An earlier study by Kipf and Welling [14] introduces Graph Autoencoder (GAE) and Variational Graph Autoencoder (VGAE), which utilize Graph Convolutional Networks (GCN) as the encoder and a dot-product decoder. These models focus on reconstructing the topological structure and node content of the graph from a compressed latent representation. ARVGA (Adversarially Regularized Variational Graph Autoencoder) [21] proposes a novel adversarial graph embedding framework. It trains a decoder to reconstruct both the topological structure and node content of the graph from a compact representation generated by the framework. This adversarial training enhances the robustness and generalization capabilities of the model. MGAE (Multi-modal Graph Autoencoder)[29] and GALA

(Graph Autoencoder with a Ladder-like Architecture)[22] are methods that combine structure and node reconstruction. They aim to learn a comprehensive representation of the graph by simultaneously reconstructing the graph structure and node attributes. In a recent study by Hou et al. [10], a graph autoencoder approach called GraphMAE is proposed, which focuses solely on node reconstruction for general graphs. By reconstructing nodes, GraphMAE achieves promising results in node classification tasks.

**Region Representation Learning.** Research on the region representation learning problem includes the following studies [5, 30, 34, 36, 38, 40, 48]. In particular, Fu et al. [5] suggest to incorporate both intra-region information (such as POI distance inside a region) and inter-region information (such as the similarity of POI distributions between two regions) to increase the quality of region representations. The concept of putting forward in [5] is expanded upon by Zhang et al. [48] by using a collective adversarial training.

In a recent study conducted by Zhang et al. [38], a multi-view joint learning model is developed to learn region representations. To capture region correlations from different perspectives, such as human mobility and region properties, the study incorporates a graph attention technique for each view. However, this approach focuses solely on modeling region correlations and does not consider the inclusion of point-of-interest (POI) data, which is essential for capturing region functionality. Similarly, Wu et al. [34] propose a method for learning area representations by extracting traffic patterns. However, their approach also excludes POI data and relies solely on mobility data. The efficacy of these techniques heavily relies on the generation of high-quality region graphs. Furthermore, they may struggle to learn accurate region representations when faced with noisy and skewed spatio-temporal data. In contrast, a recent study by Zhang et al. [40] proposes the adoption of a contrastive self-supervised learning paradigm on a multi-view heterogeneous spatio-temporal graph. This approach utilizes a self-contrastive learning method to obtain high-quality region vectors. By contrast, our paper employs a generative self-supervised learning method to model region correlations by masking links and nodes on the heterogeneous spatio-temporal graph.

## 5 CONCLUSION

We introduce a novel generative spatial-temporal graph self-supervised learning paradigm for region representation. Our approach incorporates mask mechanisms to address limitations in existing area representation methods. Through extensive experiments on real-world datasets and three spatial-temporal mining tasks, we demonstrate the effectiveness of our HGAurban in learning area graph representations from multi-view spatial-temporal data. Our contributions include proposing a self-supervised learning paradigm using generative models and masks, addressing challenges in area representation methods, and achieving superior performance compared to state-of-the-art approaches in various spatial-temporal mining tasks, such as crime prediction.

## ACKNOWLEDGEMENT

The Australian Research Council partially supports this work under the streams of Future Fellowship (Grant No. FT210100624), the Discovery Project (Grant No. DP240101108), and the Linkage

Projects (Grant No. LP230200892 and LP240200546). This project is also partially supported by Shenzhen-Hong Kong-Macao Science and Technology Plan Project (Category C Project: SGDX202108 23103537030) and Theme-based Research Scheme T35-710/20-R. We appreciate help of Dr. Huang and Dr. Xia.

## REFERENCES

- [1] Yuzhou Chen, Ignacio Segovia, and Yulia R Gel. 2021. Z-GCNets: time zigzags at graph convolutional networks for time series forecasting. In *International Conference on Machine Learning (ICML)*. PMLR, 1684–1694.
- [2] Winnie Cheng, Chris Greaves, and Martin Warren. 2006. From n-gram to skip-gram to conigram. *IJCL* 11, 4 (2006), 411–433.
- [3] Zulong Diao, Xin Wang, Dafang Zhang, Yingru Liu, Kun Xie, and Shaoyao He. 2019. Dynamic spatial-temporal graph convolutional neural networks for traffic forecasting. In *AAAI Conference on Artificial Intelligence (AAAI)*, Vol. 33. 890–897.
- [4] Zheng Fang, Qingqing Long, Guojie Song, and Kunqing Xie. 2021. Spatial-Temporal Graph ODE Networks for Traffic Flow Forecasting. In *International Conference on Knowledge Discovery and Data Mining (KDD)*. ACM, 364–373.
- [5] Yanjie Fu, Pengyang Wang, Jiadi Du, Le Wu, and Xiaolin Li. 2019. Efficient region embedding with multi-view spatial networks: A perspective of locality-constrained spatial autocorrelations. In *AAAI*, Vol. 33. 906–913.
- [6] Andrew Fuchs, Andrea Passarella, and Marco Conti. 2023. Modeling, Replicating, and Predicting Human Behavior: A Survey. *ACM Transactions on Autonomous and Adaptive Systems* (2023).
- [7] Aditya Grover and Jure Leskovec. 2016. node2vec: Scalable feature learning for networks. In *KDD*. 855–864.
- [8] Will Hamilton, Zhitao Ying, and Jure Leskovec. 2017. Inductive representation learning on large graphs. *NIPS* 30 (2017).
- [9] Kaiming He, Xinlei Chen, Saining Xie, Yanghao Li, Piotr Dollár, and Ross Girshick. 2022. Masked autoencoders are scalable vision learners. In *Proceedings of the IEEE/CVF conference on computer vision and pattern recognition*. 16000–16009.
- [10] Zhenyu Hou, Xiao Liu, Yukuo Cen, Yuxiao Dong, Hongxia Yang, Chunjie Wang, and Jie Tang. 2022. Graphmae: Self-supervised masked graph autoencoders. In *Proceedings of the 28th ACM SIGKDD Conference on Knowledge Discovery and Data Mining*. 594–604.
- [11] Jiahao Ji, Jingyuan Wang, Chao Huang, Junjie Wu, Boren Xu, Zhenhe Wu, Junbo Zhang, and Yu Zheng. 2023. Spatio-temporal self-supervised learning for traffic flow prediction. In *Proceedings of the AAAI Conference on Artificial Intelligence*, Vol. 37. 4356–4364.
- [12] Junzhong Ji, Fan Yu, and Minglong Lei. 2022. Self-Supervised Spatiotemporal Graph Neural Networks With Self-Distillation for Traffic Prediction. *IEEE Transactions on Intelligent Transportation Systems* 24, 2 (2022), 1580–1593.
- [13] Guangyin Jin, Yuxuan Liang, Yuchen Fang, Jincui Huang, Junbo Zhang, and Yu Zheng. 2023. Spatio-temporal graph neural networks for predictive learning in urban computing: A survey. *arXiv preprint arXiv:2303.14483* (2023).
- [14] Thomas N Kipf and Max Welling. 2016. Variational graph auto-encoders. *arXiv preprint arXiv:1611.07308* (2016).
- [15] Thomas N Kipf and Max Welling. 2017. Semi-Supervised Classification with Graph Convolutional Networks. In *ICLR*.
- [16] Mengzhang Li and Zhanxing Zhu. 2021. Spatial-temporal fusion graph neural networks for traffic flow forecasting. In *AAAI*, Vol. 35. 4189–4196.
- [17] Sihang Li, Xiang Wang, An Zhang, Yingxin Wu, Xiangnan He, and Tat-Seng Chua. 2022. Let invariant rationale discovery inspire graph contrastive learning. In *ICML*. PMLR, 13052–13065.
- [18] Jiawei Liu, Haihan Gao, Chuan Shi, Hongtao Cheng, and Qianlong Xie. 2023. Self-Supervised Spatio-Temporal Graph Learning for Point-of-Interest Recommendation. *Applied Sciences* 13, 15 (2023), 8885.
- [19] Jing Long, Tong Chen, Quoc Viet Hung Nguyen, and Hongzhi Yin. 2023. Decentralized collaborative learning framework for next POI recommendation. *ACM Transactions on Information Systems* 41, 3 (2023), 1–25.
- [20] Zhongjian Lv, Jiajie Xu, Kai Zheng, Hongzhi Yin, Pengpeng Zhao, and Xiaofang Zhou. 2018. Lc-rnn: A deep learning model for traffic speed prediction. In *IJCAI*, Vol. 2018. 27.
- [21] Shirui Pan, Ruiqi Hu, Guodong Long, Jing Jiang, Lina Yao, and Chengqi Zhang. 2018. Adversarially regularized graph autoencoder for graph embedding. *arXiv preprint arXiv:1802.04407* (2018).
- [22] Jiwoong Park, Minsik Lee, Hyung Jin Chang, Kyuewang Lee, and Jin Young Choi. 2019. Symmetric graph convolutional autoencoder for unsupervised graph representation learning. In *Proceedings of the IEEE/CVF international conference on computer vision*. 6519–6528.
- [23] Alex Pentland and Andrew Liu. 1999. Modeling and prediction of human behavior. *Neural computation* 11, 1 (1999), 229–242.
- [24] Hossein A Rahmani, Mohammad Aliannejadi, Rasoul Mirzaei Zadeh, Mitra Baratchi, Mohsen Afsharchi, and Fabio Crestani. 2019. Category-aware location embedding for point-of-interest recommendation. In *SIGIR*. 173–176.
- [25] Zahraa Al Sahili and Mariette Awad. 2023. Spatio-Temporal Graph Neural Networks: A Survey. *arXiv preprint arXiv:2301.10569* (2023).
- [26] Amin Salehi and Hasan Davulcu. 2019. Graph attention auto-encoders. *arXiv preprint arXiv:1905.10715* (2019).
- [27] Xuxiang Ta, Zihan Liu, Xiao Hu, Le Yu, Leilei Sun, and Bowen Du. 2022. Adaptive spatio-temporal graph neural network for traffic forecasting. *Knowledge-Based Systems* 242 (2022), 108199.
- [28] Petar Veličković, Guillem Cucurull, Arantxa Casanova, Adriana Romero, Pietro Lio, and Yoshua Bengio. 2018. Graph attention networks. In *ICLR*.
- [29] Chun Wang, Shirui Pan, Guodong Long, Xingquan Zhu, and Jing Jiang. 2017. Mgae: Marginalized graph autoencoder for graph clustering. In *Proceedings of the 2017 ACM on Conference on Information and Knowledge Management*. 889–898.
- [30] Hongjian Wang and Zhenhui Li. 2017. Region representation learning via mobility flow. In *CIKM*. 237–246.
- [31] Xiaoyang Wang, Yao Ma, Yiqi Wang, Wei Jin, Xin Wang, Jiliang Tang, et al. 2020. Traffic flow prediction via spatial temporal graph neural network. In *The Web Conference (WWW)*. 1082–1092.
- [32] Yuandong Wang, Hongzhi Yin, Hongxu Chen, Tianyu Wo, Jie Xu, and Kai Zheng. 2019. Origin-destination matrix prediction via graph convolution: A new perspective of passenger demand modeling. In *Proceedings of the 25th ACM SIGKDD international conference on knowledge discovery & data mining*. 1227–1235.
- [33] Yuandong Wang, Hongzhi Yin, Lian Wu, Tong Chen, and Chunyang Liu. 2021. Secure your ride: Real-time matching success rate prediction for passenger-driver pairs. *IEEE Transactions on Knowledge and Data Engineering* 35, 3 (2021), 3059–3071.
- [34] Shangbin Wu, Xu Yan, Xiaoliang Fan, Shirui Pan, Shichao Zhu, Chuanpan Zheng, Ming Cheng, and Cheng Wang. 2022. Multi-Graph Fusion Networks for Urban Region Embedding. In *IJCAI*.
- [35] Lianghao Xia, Chao Huang, Yong Xu, Peng Dai, Liefeng Bo, Xiyue Zhang, and Tianyi Chen. 2021. Spatial-Temporal Sequential Hypergraph Network for Crime Prediction with Dynamic Multiplex Relation Learning. In *IJCAI*. 1631–1637.
- [36] Zijun Yao, Yanjie Fu, Bin Liu, Wangsu Hu, and Hui Xiong. 2018. Representing urban functions through zone embedding with human mobility patterns. In *IJCAI*.
- [37] Yuning Yu, Tianlong Chen, Yongduo Sui, Ting Chen, Zhangyang Wang, and Yang Shen. 2020. Graph contrastive learning with augmentations. *NeurIPS* 33 (2020), 5812–5823.
- [38] Mingyang Zhang, Tong Li, Yong Li, and Pan Hui. 2021. Multi-view joint graph representation learning for urban region embedding. In *IJCAI*. 4431–4437.
- [39] Qianru Zhang, Xinyi Gao, Haixin Wang, Siu Ming Yiu, and Hongzhi Yin. 2025. Efficient traffic prediction through spatio-temporal distillation. In *Proceedings of the AAAI Conference on Artificial Intelligence*, Vol. 39. 1093–1101.
- [40] Qianru Zhang, Chao Huang, Lianghao Xia, Zheng Wang, Zhonghang Li, and Siuming Yiu. 2023. Automated Spatio-Temporal Graph Contrastive Learning. In *Proceedings of the ACM Web Conference 2023*. 295–305.
- [41] Qianru Zhang, Chao Huang, Lianghao Xia, Zheng Wang, Siu Ming Yiu, and Ruihua Han. 2023. Spatial-Temporal Graph Learning with Adversarial Contrastive Adaptation. In *International Conference on Machine Learning*. PMLR, 41151–41163.
- [42] Qianru Zhang, Haixin Wang, Cheng Long, Liangcai Su, Xingwei He, and Jianlong Chang, Tailin Wu, Hongzhi Yin, Siu-Ming Yiu, Qi Tian, and Christian S. Jensen. 2024. A Survey of Generative Techniques for Spatial-Temporal Data Mining. *arXiv preprint arXiv:2405.09592* (2024).
- [43] Qianru Zhang, Haixin Wang, Cheng Long, Liangcai Su, Xingwei He, Jianlong Chang, Tailin Wu, Hongzhi Yin, Siu-Ming Yiu, Qi Tian, et al. 2024. A survey of generative techniques for spatial-temporal data mining. *arXiv preprint arXiv:2405.09592* (2024).
- [44] Qianru Zhang, Zheng Wang, Cheng Long, Chao Huang, Siu-Ming Yiu, Yiding Liu, Gao Cong, and Jieming Shi. 2023. Online anomalous subtrajectory detection on road networks with deep reinforcement learning. In *2023 IEEE 39th International Conference on Data Engineering (ICDE)*. IEEE, 246–258.
- [45] Qianru Zhang, Honggang Wen, Ming Li, Dong Huang, Siu-Ming Yiu, Christian S Jensen, and Pietro Liò. 2025. AutoHFormer: Efficient Hierarchical Autoregressive Transformer for Time Series Prediction. *arXiv preprint arXiv:2506.16001* (2025).
- [46] Qianru Zhang, Peng Yang, Junliang Yu, Haixin Wang, Xingwei He, Siu-Ming Yiu, and Hongzhi Yin. 2025. A survey on point-of-interest recommendation: Models, architectures, and security. *IEEE Transactions on Knowledge and Data Engineering* (2025).
- [47] Qianru Zhang, Chenglei Yu, Haixin Wang, Yudong Yan, Yuansheng Cao, Siu-Ming Yiu, Tailin Wu, and Hongzhi Yin. 2025. FLDmamba: Integrating Fourier and Laplace Transform Decomposition with Mamba for Enhanced Time Series Prediction. *arXiv preprint arXiv:2507.12803* (2025).
- [48] Yunchao Zhang, Yanjie Fu, Pengyang Wang, Xiaolin Li, and Yu Zheng. 2019. Unifying inter-region autocorrelation and intra-region structures for spatial embedding via collective adversarial learning. In *KDD*. 1700–1708.